

## Fabrication and Biofunctionalization of Carbon-Encapsulated Au Nanoparticles

Nitin Chopra,<sup>†</sup> Leonidas G. Bachas,<sup>‡</sup> and Marc R. Knecht<sup>\*‡</sup>

Department of Chemistry, University of Kentucky, Lexington, Kentucky 40506-0055, and Metallurgical and Materials Engineering Department, Center for Materials for Information Technology (MINT), University of Alabama, Tuscaloosa, Alabama 35487

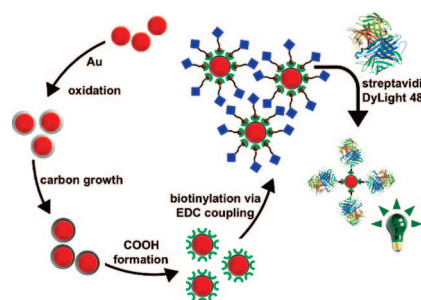
Received December 11, 2008

Revised Manuscript Received March 7, 2009

Au nanoparticles (AuNPs) are used in a variety of applications because of their small size and size-dependent optical properties, thus positioning them as important components of biological and chemical sensors.<sup>1</sup> Most AuNP sensing systems use discrete particle aggregation in response to biological elements, which results in a measurable color change. Their detection level is relatively low with a high degree of sensitivity.<sup>1</sup> While the interest in such sensors has increased, the ability to use AuNPs in biological systems is limited due to particle stability and nonspecific binding. These limitations are more pronounced in high ionic strength media, such as those used for biological assays.<sup>2</sup> The subsequent nanoparticle aggregation can yield bulk materials and/or false positive results, both of which are undesirable. These negative aspects strongly depend on the type of ligand used to passivate the AuNP surface; these ligands can be displaced or cross-linked due to the multitude of ionic species present in the solution.<sup>1</sup>

A variety of methods for nanoparticle surface passivation have been developed.<sup>1,3–5</sup> An emerging method that involves the use of a carbon nanoshell encapsulating the metal particle has shown great promise.<sup>3,6</sup> Additionally, carbon nanomaterials have been recently investigated for biological applications.<sup>7</sup> Carbon shells have been used to prevent chemical modification of reactive and/or oxidizable nanomaterials such as Fe, Ge, Ni, and GaN.<sup>3,8–10</sup> Graphene-like carbon shells act as superior surface passivants as compared to standard ligands; however,

**Scheme 1. Representative Scheme Designed for the CVD-Based Synthesis of Au@C Nanoparticles on a Si Substrate**



in some cases the carbon reacts with the metal core resulting in metal carbides.<sup>11</sup> To this end, encapsulation of noble metals like Au, which are typically not capable of catalyzing the production of carbon materials, in a graphene-like carbon shell is ideal as it is nonreactive with the metallic surface and provides unsurpassed stability, while possessing a convenient handle for functionalization.<sup>12</sup> The only convenient method for the growth of carbon shells on AuNPs is limited to carbon deposition during transmission electron microscopic (TEM) analysis.<sup>5,10</sup> While the desired Au-core carbon-shell (Au@C) structure is fabricated, only minute quantities of the materials are produced where subsequent separation and use of the materials is nearly impossible. For future applications of Au@C nanoparticles, the materials must be produced in sufficient quantities and functionalized in an efficient manner.

Herein, we report the fabrication of Au@C nanoparticles using a facile chemical vapor deposition (CVD) synthesis and their potential application in bioanalysis. These materials are highly robust and can be produced with a controlled thickness of a graphene-like carbon shell. Dispersed and plasma-oxidized AuNPs on chemically modified Si substrates were used as catalysts for carbon growth. Silane chemistry was used to covalently attach the AuNPs on the Si substrate.<sup>13</sup> In a typical experiment, Scheme 1, “piranha” cleaned Si substrates were immersed in a 12.4 mM solution of 3-mercaptopropyltrimethoxy silane (MPTMS) in EtOH and stirred gently for 24 h. After silanization, the substrates were rigorously cleaned in EtOH and immersed in a 5% aqueous AuNP solution for 24 h, which linked the AuNPs onto the substrates. Finally, the substrates were washed in EtOH, dried under Ar, and stored in a vacuum oven. The AuNPs on Si substrates were oxidized in an O<sub>2</sub> plasma process (O<sub>2</sub> flow, 20–30 sccm; power, 100 W; and pressure, 300 mTorr) for 15 min. Dispersed AuNPs were plasma oxidized to remove the initial citrate surface passivant and to partially form gold oxide on the surface,<sup>14</sup> which is critical to

\* To whom correspondence should be addressed. Tel.: (859) 257-3789. E-mail: mrknecht2@email.uky.edu (M.R.K.), nchopra@eng.ua.edu (N.C.), bachas@uky.edu (L.G.B.).

<sup>†</sup> University of Alabama.

<sup>‡</sup> University of Kentucky.

- (1) Rosi, N. L.; Mirkin, C. A. *Chem. Rev.* **2005**, *105*, 1547–1562. (b) Daniel, M.-C.; Astruc, D. *Chem. Rev.* **2004**, *104*.
- (2) Sethi, M.; Joung, G.; Knecht, M. R. *Langmuir* **2009**, *25*, 317–325.
- (3) Krashennnikov, A. V.; Banhart, F. *Nat. Mater.* **2007**, *6*.
- (4) Ma, J.; Hu, Z.; Yu, L.; Hu, Y.; Yue, B.; Wang, X.; Chen, Y.; Lu, Y.; Liu, Y.; Hu, J. *J. Phys. Chem. B* **2006**, *110*.
- (5) Sutter, E.; Sutter, P.; Zhu, Y. *Nano Lett.* **2005**, *5*, 2092–2096.
- (6) Kim, M.; Sohn, K.; Na, H. B.; Hyeon, T. *Nano Lett.* **2002**, *2*, 1383–1387.
- (7) (a) Liu, Z.; Winters, M.; Holodniy, M.; Dai, H. *Angew. Chem., Int. Ed.* **2007**, *46*, 2023–2027. (b) Rege, K.; Viswanathan, G.; Zhu, G.; Vijayaraghavan, A.; Ajayan, P. M.; Dordick, J. S. *Small* **2006**, *2*, 718–722.
- (8) Geng, J.; Jefferson, D. A.; Johnson, F. G. *Chem. Commun.* **2004**, 2442–2443.
- (9) Sutter, E.; Sutter, P.; Calarco, R.; Stoica, T.; Meijers, R. *Appl. Phys. Lett.* **2007**, *90*, 093118/1–3.
- (10) Sutter, E.; Sutter, P. *Adv. Mater.* **2006**, *18*, 2583–2588.

- (11) Ruoff, R. S.; Lorents, D. C.; Chan, B.; Malhotra, R.; Subramoney, S. *Science* **1993**, *259*, 346–348.
- (12) Meyyapan, M. *Carbon Nanotubes: Science and Applications*; CRC Press: Boca Raton, FL, 2005.
- (13) Slawinski, G. W.; Zamborini, F. P. *Langmuir* **2007**, *23*, 10357–10365.
- (14) Tsai, H.; Hu, E.; Perng, K.; Chen, M.; Wu, J.-C.; Chang, Y.-S. *Surf. Sci.* **2003**, *537*, L447–L450.

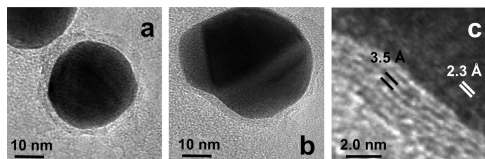


**Figure 1.** TEM images of Au@C nanoparticles after of 1.0 h CVD growth. Part (c) displays a high-resolution image of the carbon shell.

the formation of the carbon shells (*vide infra*).<sup>15</sup> Carbon shells were then grown on the oxidized AuNPs using a CVD process (1–4 h growth duration, 725 °C) as reported earlier, in the absence of a secondary catalyst.<sup>16</sup> Once grown, the carbon shell was partially oxidized, in a similar O<sub>2</sub> plasma process,<sup>17</sup> from which the materials can be removed from the Si surface via sonication.

Using 1.0 h CVD growth conditions, a carbon shell of ~1.2–2.8 nm was formed on the oxidized AuNP surface, as shown in Figure 1 and in the Supporting Information, Figure S2. The shell contains ~5–9 independent graphene layers, with an interplanar spacing of  $0.34 \pm 0.01$  nm, which is consistent with *c*-axis spacing of graphene sheets in graphite.<sup>12</sup> As observed, the AuNPs increased in size after carbon encapsulation. Prior reports indicate that electron beam irradiation can cause coalescence of AuNPs that are separated by a distance of ~1 nm within 2 min.<sup>5</sup> Although our AuNPs were not exposed to such an intense treatment and were uniformly dispersed (separation:  $135 \pm 113$  nm; Supporting Information, Figure S1), some degree of AuNP coalescence occurred. This can be due to the plasma oxidation process and/or the longer carbon growth durations, which can lead to surface migration of the AuNPs. On the basis of particle surface density,  $\sim 2.5 \times 10^7$  Au@C nanoparticles/mm<sup>2</sup> can be produced using this approach.

To demonstrate our ability to control the thickness of the carbon shell, we varied the CVD growth time. Using longer growth durations, formation of a thicker carbon shell was observed (Supporting Information, Figure S3). The average shell thickness increased linearly with the growth time at a rate of ~8 nm/h. At durations of  $\geq 4$  h, rupturing of the carbon shells was observed, dissociating them from the AuNP core. It is likely that prolonged exposure to the harsh conditions caused fissures in the graphene shell leading to weakened regions in the material. As the thermal process ensued, these regions become progressively weaker, resulting in full shell rupture and subsequent AuNP release. As a result, carbon growth durations of <4.0 h were used to avoid sample degradation. Moreover, there was negligible amorphous carbon deposition throughout the process. Similar observations have been made in the case of TEM-based synthesis of carbon shells on template AuNPs; however, the template release was observed at a very short duration (2–8 min) and was attributed to the surface tension and pressure of the AuNPs due to the growing number of carbon shells.<sup>5</sup>

To understand the process for the growth of the carbon shell on a typically inert noble metal surface, an extensive set of reaction and characterization experiments were conducted as presented in the Supporting Information, Figure S4. Initially, the formation of the Au@C structure was studied on fully reduced (i.e., nonsurface oxidized) AuNPs immobilized on a Si substrate. When these nonoxidized materials were subjected to the CVD growth conditions described above, no evidence of a carbon-shell was observed. TEM analysis of these materials after CVD growth conditions demonstrated only slightly agglomerated AuNPs. We then decided to follow a similar process but used surface-oxidized AuNPs rather than the fully reduced species. This was prompted by the fact that recent results demonstrated production of single-walled carbon nanotubes (CNTs) from an oxidized, and subsequently in situ H<sub>2</sub> reduced, AuNP source.<sup>18</sup> In this experiment, AuNPs were covalently linked to the Si surface and subsequently surface oxidized. TEM analysis of these materials displayed slightly agglomerated AuNPs due to surface migration of the materials during oxidation. Note that dispersing the materials evenly on the surface produced a uniform and large interparticle distance, thus minimizing the agglomeration process. The oxidation depth was unable to be resolved using high resolution TEM, indicating that only a minor fraction of the material's surface was actually oxidized. After CVD growth conditions, formation of a carbon-shell was evident. From TEM analysis of these materials, 100% of the observed AuNPs possessed a carbon-shell, indicating that partial oxidation of the AuNP surface is required to catalyze the carbon growth (Supporting Information, Figures S2–S4).<sup>15</sup>

While it was surprising that the formation of the carbon-shell was observed only when surface oxidized AuNPs were used, previous results have demonstrated CNT growth using an oxidized AuNP source that was subsequently reduced in situ using H<sub>2</sub>.<sup>18</sup> The process developed here uses a similar H<sub>2</sub>-based environment; however, it is likely that nanoshells were fabricated, rather than nanotubes, due to differences in CVD growth conditions: xylenes were used for nanoshell production at 725 °C, while a mixture of C<sub>2</sub>H<sub>4</sub> and CH<sub>4</sub> produced CNTs at 800–900 °C.<sup>18</sup> Further studies on the duration of oxidation of the AuNPs demonstrated varying results. No shell formation was observed when AuNPs were oxidized for  $\leq 10.0$  min. When oxidation durations in excess of 10.0 min were used, the Au@C structure was consistently observed. For all subsequent carbon growth processes, an initial AuNP oxidation time of 15.0 min was used as this duration reproducibly generated the Au@C structure with the smallest level of nanoparticle surface agglomeration. Severe particle coalescence was observed for materials that were plasma oxidized for longer time periods, thus producing a less desirable sample.

Since previous results demonstrated Au@C formation using electron beam irradiation during TEM analysis,<sup>5,10</sup> we were concerned that the results observed may be due to the TEM analysis. While our TEM conditions were at significantly lower temperatures as compared to the previous studies,<sup>5,9,10</sup> a different AuNP surface was used, an oxidized AuNP versus a fully reduced AuNP, which may result in shell formation. To confirm

(15) Hore, S.; Kaiser, G.; Hu, Y.-S.; Schulz, A.; Konuma, M.; Gotz, G.; Sigle, W.; Verhoeven, A.; Maier, J. *J. Mater. Chem.* **2008**, *18*, 5589–5591.

(16) Andrews, R.; Jacques, D.; Rao, A. M.; Derbyshire, F.; Qian, D.; Fan, X.; Dickey, E. C.; Chen, J. *Chem. Phys. Lett.* **1999**, *303*, 467–474.

(17) Hinds, B. J.; Chopra, N.; Rantell, T.; Andrews, R.; Gavalas, V. G.; Bachas, L. G. *Science* **2004**, *303*, 62–65.

(18) Bhaviripudi, S.; Mile, E.; Steiner, S. A., III; Zare, A. T.; Dresselhaus, M. S.; Belcher, A. M.; Kong, J. *J. Am. Chem. Soc.* **2007**, *129*, 1516–1517.

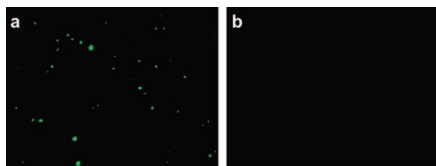


**Figure 2.** Fluorescence microscopy images of (a) biotinylated and (b) nonbiotinylated Au@C nanoparticles after streptavidin incubation.

that our shell was indeed grown during the CVD process and not during TEM imaging, surface-oxidized AuNPs were exposed to the electron beam of the TEM for long durations of >30 min. As is consistent with the above-described CVD process, formation of a carbon shell was never observed under electron beam irradiation using standard TEM conditions, suggesting that carbon growth occurred only during the CVD process. Taken together these results demonstrate that carbon-shell formation is dependent upon an oxidized Au surface and the duration of the CVD growth process. Other factors affecting the synthesis include the quality of carbon feed, growth temperature, surface defects on the AuNPs, and the size and shape of the AuNPs.

As a result of the enhanced process developed herein for the production of Au@C materials, a higher number of particles can be fabricated in a method that is predisposed for facile surface functionalization. With such advantages, the functionalization process can be fine-tuned for bioanalytical purposes. AuNPs are intrinsically sensitive to solution ionic strength and nonspecific binding of biomacromolecules, which can prevent their use under traditional biological conditions.<sup>2</sup> On the basis of the Au@C structure, the nanoparticles demonstrate a high degree of stability. Particle agglomeration was halted once shell formation began, which is evident by only individual Au@C nanoparticles observed rather than a network of intermixed Au and carbon materials. With the Au@C core-shell structure, nanoparticle stability is increased; however, functionalization of the surface is required for their application. One method, graphene plasma oxidation, produces surface -COOH functionalities,<sup>17</sup> which serve as handles for molecular attachment.

To demonstrate the bioanalytical capabilities of the Au@C nanoparticles with shell thickness of ~10 nm, plasma oxidation of the carbon shells was used. This process etched away ~1 nm of the shell, resulting in -COOH functionalities displayed on the surface. Such functional groups are ideal and have previously been used for attachment of biologically relevant species.<sup>17</sup> The well-established biotin/streptavidin (DyLight 488 labeled) binding system was chosen as a model example of biofunctionalization of the Au@C system. Biotin was conjugated onto the carbon surface using standard carbodiimide chemistry.<sup>17</sup> The resulting structure, which remained immobilized on the Si surface, now presented numerous biotin molecules to solution. This arrangement facilitated the binding of the DyLight 488-labeled streptavidin. On the basis of an Au@C diameter of 28 nm and streptavidin dimensions,<sup>19</sup> a

maximum of 7–8 proteins can bind to the surface. The bound and highly fluorescent protein was utilized to locate the functionalized Au@C nanoparticles on the Si substrate using fluorescence microscopy. The materials remained immobilized on the Si substrate to allow for imaging of the fluorescently tagged structures. As shown in Figure 2a bright green fluorescence was identified on the Si surface in areas where the biotinylated Au@C structure is located. The size of the fluorescent region is larger than the actual particle size due to light scattering and the limit of optical detection.

To confirm that the observed fluorescence emission was the result of targeted biological events, rather than nonspecific adsorption of the tagged protein, a series of control experiments were performed (Supporting Information, Figure S5). The controls included native Au@C nanoparticles, surface immobilized bare AuNPs, and a blank Si substrate. Each of these samples was subjected to the biotinylation process employed previously and washed with copious amounts of deionized water. For all controls, no -COOH functionalities are expected to be present; therefore, incorporation of the biotin molecule is unlikely. Fluorescence analysis demonstrated that each sample possessed no observable fluorescence emission. Only Au@C nanoparticles with oxidized carbon shells displayed green fluorescence (Figure 2a), while Au@C nanoparticles with nonoxidized carbon shell (Figure 2b), AuNPs, and a blank Si substrate were fluorescently silent. Such results confirm the viability of surface functionalization of the Au@C nanoparticles and that their potential use in biological systems is both possible and promising. Additionally, these control studies indicate that nonspecific binding of the protein was minimal for all nanomaterial species as no fluorescence from any of the nonbiotinylated structures was observed. This suggests that the Au@C surface is well suited for biological applications with minimal background noise.

In summary, we have developed a scheme for the fabrication of Au@C nanoparticles using a CVD process. Such a technique represents an advance in the production of an addressable quantity of materials for bioanalytical applications; however, further enhancement is required. The materials are highly robust and are readily functionalizable for a variety of biobased applications. Of significant note, these materials also demonstrate a minimal degree of nonspecific binding, which is desirable for their application in biological assays. Such results are intriguing for bioanalytical applications, which are presently under study.

**Acknowledgment.** We thank U. Kentucky for financial support, Dr. Andrews and Qian (CAER) for carbon growth, CeNSE for instrument support, and the Microscopy Center for EM assistance. We thank Dr. J.Z. Hilt for access to the fluorescence analysis. N.C. and L.G.B. acknowledge funding from the National Aeronautics and Space Administration.

**Supporting Information Available:** Experimental section and additional characterization (PDF). This information is available free of charge via the Internet at <http://pubs.acs.org>.

CM803349C

(19) Caswell, K. K.; Wilson, J. N.; Bunz, U. H. F.; Murphy, C. J. *J. Am. Chem. Soc.* **2003**, *125*, 13914–13915.